Synthesis and Characterization of Activated Carbons from Walnut Shells to Remove Diclofenac

Bougheriou, Fatima; Ghoualem, Hafida*+

USTHB, Laboratory of Electrochemistry-Corrosion, Metallurgy and Mineral Chemistry. Faculty of Chemistry, University of Sciences and Technology Houari Boumediene. 16111 Bab-Ezzouar Algiers, ALGERIA

ABSTRACT: *Diclofenac batch adsorption was investigated in a synthesized aqueous solution using Activated Carbons (ACs) prepared from walnut shells with the chemical activation method. The use of phosphoric acid as an activating agent for preparing of ACs has been studied. The ACs were yielded at various concentrations 20,35,40,60,75 and 85%, respectively, which are termed AC20, AC35, AC40, AC60, AC75 and AC85%. Adsorbent was characterized for its texture by Scanning Electron Microscopy, Granulomere laser, Interferometric Microscopy, X-ray diffraction and Fourier transform infrared spectroscopy-Attenuated total reflectance. The structure determined by the iodine and methylene blue number, point of zero charge measurement and optimization of diclofenac adsorption parameters. The adsorbate was determined by adsorption tests were performed on diclofenac sodium by varying the mass of ACs, pHi, initial concentration, stirring speed, contact time and temperature. The limits of pharmaceutical substance adsorption by prepared ACs were 99.66% with AC35% at pH= 2, m35% = 2mg, at contact time of 60min for diclofenac sodium. The synthesis results showed that the optimal physicochemical properties of the ACs were observed at 25°C, optimal iodine and methylene blue adsorption of AC35% was 3784.6 mg/g and 1990.67 mg/g, respectively. It was observed that the removal efficiency of Diclofenac sodium (DCF) was defined by the reactivity with the adsorbent and the percentage of activating agent. The ACs elaborate are an excellent adsorbent for the removal of the pharmaceutical substance studied.*

KEYWORDS*: Walnut shells; Activated carbon; Chemical activation; Adsorption.*

INTRODUCTION

Activated carbon is a porous carbon material with high adsorption ability, it is extensively used in various applications. These applications cover a vast range of systems, including water and wastewater treatment, separations, hazardous waste treatment, industrial wastewater and gas treatment as an adsorbent due to its large specific surface area, reactivation property, desired porous structure, good chemical resistance and various oxygen-containing functional groups on its surface. Nowadays, AC can be produced from a huge number of accessible and inexpensive materials containing high carbon content and low inorganic content, such as apricot

*****To whom correspondence should be addressed.*

+ *E-mail: hghoualem@usthb.dz*

1021-9986/2023/9/2834-2854 21/$/7.01

stones, coconut shell, cherry pit, rice husk, peanut shell, walnut shell [1-5]. The main production process of activated carbon is focused on the activation and carbonization of the raw material [6]. The activation of precursor can be implemented either physically or chemically. A typical physical method consists of a thermal treatment that is carried out in two steps: first is carbonization of the precursor and the second is controlled gasification (steam flow, temperature, heating rate, etc.) of the raw material. In the chemical method, the feedstock is impregnated with a chemical agent, such as KOH, NaOH, K_2CO_3, $ZnCl_2$, $FeCl_3$, H_2SO_4, and H_3PO_4, and the mixture is heated to a temperature of 450-700 °C [7]. The chemical activation reduces the formation of tar and other byproducts thus increasing the carbon yield. The type and number of chemical agents used are important to improve the quality and quantity of the activated carbon obtained [8].

Activated carbons are of interest in many economic sectors and concern many industries as diverse as food processing, pharmaceuticals, chemical, petroleum, mining, nuclear, automobile and vacuum manufacturing.

The physicochemical characteristics of activated carbon depend on the type of raw material used and activation conditions. Activated carbons are classified into one of three types, such as powder, granular and fibers, according to their size and shape, and each type has its specific application. Raw materials for activated carbon are chosen according to their purity, price, potential degree of activation, and stability of supply. They derive their adsorptive properties from an extensive internal porous structure that has a high surface area available for adsorption of molecular species. This high porosity is a function of both the precursor and the activation scheme. The precursors to activated carbons are either of botanical origin (wood, coconut and nut shells) or degraded and charred plant material (peat, lignite and all types of coal). Agricultural wastes are considered very important raw materials due to two facts: they are renewable sources and inexpensive materials. In recent years, condensed research on activated carbons from agricultural residues has been reported (apricot pits, peach pits, cherry pits, date pits, wheat straw, pecan shells, hulls of soybean and rice), walnut shells and many others (grape seeds, plum stones, almond shells), corncobs have received very little mention, even though they are a cheap and abundant agricultural waste product with no economic value [9–11].

Phosphoric acid and zinc chloride are used for the activation of lignocellulosic materials that have not been previously carbonized, while metal compounds such as potassium hydroxide are used for the activation of coal or biochar precursors. Compared to zinc chloride, phosphoric acid is most preferred because of the environmental drawbacks associated with zinc chloride.

In addition, carbons obtained with zinc chloride cannot be used in the pharmaceutical and food industries because they contaminate the product [12]. Thus, the researchers focused on the production of activated carbon from biomass and renewable natural sources as an alternative to fully utilizing these resources [13-19]. Diclofenac (DCF) is an anti-inflammatory non-steroidal drug. Its sodium salt has been widely used in medical care as an analgesic, antiarthritic and antirheumatic reagent with a high consumption rate [20]. High concentrations of diclofenac in wastewater are a significant problem for the environment. owing to incomplete removal of DCF by conventional wastewater treatment processes [20-21]. The contamination of water resources by DCF can cause poisoning and decline in the population of birds, fish and aquatic creatures. This poisoning effect can even increase when a mixture of DCF with other pharmaceuticals is used [22]. It has been confirmed as a persistent pollutant due to its low biodegradability and sorption properties, can transform into very toxic metabolites [23-24]. The study of the environmental behavior of pharmaceuticals, some technics such as membrane filtration [25], adsorption [26], chemical treatment, and Advanced Oxidation Process (AOP) [27], etc. They have been used to minimize the concentration of DCF or other pollutants in water. Most of these traditional techniques have some disadvantages, such as expensiveness, need to advanced techniques or equipment, remaining the pollutants because they may transfer the concomitant from one phase to another, etc. [28].

In this research, walnut shells were used as a precursor for the production of activated carbons by chemical activation with phosphoric acid, due to its cost effectiveness, it is used as an activating agent for producing activated carbons. The effects of the different concentrations of H_3PO_4 on the properties of activated carbons were investigated. They explored the effects of physicochemical parameters of ACs prepared including

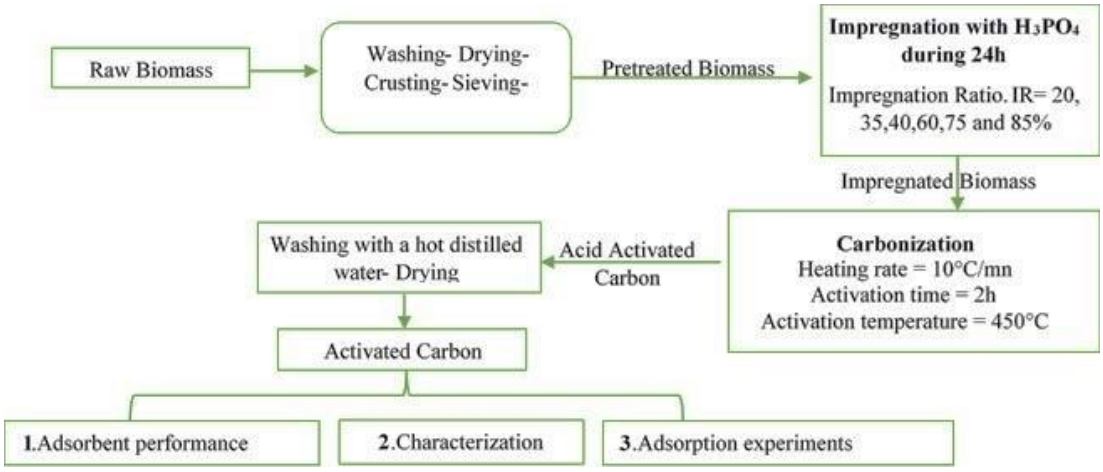

Fig.1: The preparation process of activated carbon

pH, adsorbent dosage, and initial DCF concentration, as well as the impacts of contact time and temperature on DCF removal process in a batch system. Then, a comparison of the diclofenac sodium absorption capacity of activated carbon was performed to study the yield of removal. In addition, the results of Fourier Transform InfrarRed (FT-IR) spectroscopy, X-Ray powder Diffraction (XRD), Scanning Electron Microscopy (SEM-EDS), particle size distributions and interferometric microscopy were used to characterize the structure and morphology of the adsorbents in order to find the physicochemical properties of ACs at different concentrations and its feasibility for application in the adsorption of this drug residue were investigated and discussed. The advantages of chemical activation are low energy cost, since chemical activation generally takes place at a lower temperature than that used in physical activation, and the yields of chemical activation are higher than those of physical activation [29,30]. Chemical activation also allows for better development of a porous structure [31].

EXPERIMENTAL SECTION

Preparation of activated carbons

In this study, the walnut shells used were collected from agriculture waste, and are originally from the area of Cheliff Algeria. They were washed with water several times to remove dust until clear water was obtained. Then, the shells were rinsed with distilled water and dried at 110°C for 24 hours. The dried samples were crushed and sieved to a size of about 0.5 mm, this powder fraction was used for the preparation of activated carbon. The proximal analysis of the precursor according to the AC standards based on to SNI standards of (06-3730-1995) have shown that these agricultural wastes are considered good candidate for conversion to activated carbon due to their relatively high carbon content and low ash content **[6].**

The chemical activation of the powdered precursor was performed using phosphoric acid (H_3PO_4) (Fig.1). Thus, several aqueous solutions of H_3PO_4 were prepared at 20, 35, 40, 60, 75, and 85% by weight. 10g of dried precursor was mixed with 20 mL of each solution. The mixing was performed at 25°C for 24 hours. After mixing, the suspension was subjected to vacuum drying (oven MEMMERT) at 110°C for 24 hours. The obtained samples were washed with hot distilled water several times until the filtrate reached a neutral pH. The resulting sample was dried at 110°C for 24 hours. Finally, the chemically activated samples were placed in a muffle furnace at 450°C at a heating rate of 10°C/min for 2 hours.

Characterization of activated carbons

The physicochemical characteristics of the activated carbon were determined by several techniques and different analysis

Proximate analysis of carbon produced

The ACs were subjected to characterization in order to test it for properties like moisture content, volatile matter, ash content, and fixed carbon. The ash content was determined in accordance using the procedure of ASTM D2866-94 (2000), moisture content was determined according to ASTM D3173-00 while the volatile matter according to

ASTM D1762-84 (2007), and Fixed carbon is a measure of the amount of non-volatile carbon remaining in a coal sample. It is a calculated value determined from other parameters measured in approximate analysis, rather than through direct measurement (ASTM method D3172-07a, American Society for Testing and Materials, 2013, p. 492-493). Fixed carbon is the calculated percentage of material lost in the moisture, volatile matter, and ash tests from the following formulas:

Moisture content % = (Weight reduced/Weight be foreheating at oven) * 100%. (1)

Volatile Matter % = (Weight reduced/ Weight of furnace-dried samples) * 100%. (2)

Ash % = Weight of Ash/Weight of furnace-dried samples) *100%. (3)

Fixed carbon % = 100%-(Moisture%+Volatile Matter%+Ash%). (4)

Point of Zero Charge pH (pH_{PZC}) measurement

The pHpzc value characterizes surface acidity. When oxide particles are introduced in an aqueous environment, their surface charge is positive if pH (solution)is <pHpzc and it is negative if pH (solution) is >pHpzc. The pH_{PZC} (the pH value at which the surface has zero net charge) was determined by the so-called pH derivative method **[32].** The pH of aqueous NaCl solutions was adjusted to successive initial values between 2 and 12 by adding either 0.1M of HCl or 0.1M of NaOH. Mixtures were prepared by adding the optimal mass of each activated carbon to each solution. The final pH was measured and plotted against the initial pH after 24 hours of stirring. The pH_{PZC} was determined at the value for which pH_{final} is equal to $pH_{initial}$.

Iodine number

The iodine number is the magnitude of iodine absorbed by 1 g of carbon. The iodine number can be acclimated to estimate the surface area and microporosity of activated carbons with good precision which defines the small pore (<2 nm) of an activated carbon and therefore reflects its ability to adsorb small substances. To determine the iodine number, a volume of HCl 5% by weight was added to a quantity of activated carbon, swirled until the carbon was wetted, then the volume of 0.1 N iodine solution was added and the content was shaken vigorously for a few minutes then filtered. The 10 mL of filtrate was titrated with sodium thiosulfate using starch as indicator (ASTM 2006) [33].

The iodine number was calculated using the following equation:

$$I_2N\left(\frac{mg}{g}\right)=\frac{(C_0I_2-\frac{C_{Na_2S_2O_3}.V_{Na_2S_2O_3}}{2V_{I_2}}).M_{I_2}.V_{ads}}{m_{AC}} \quad (5)$$

Where, C_0I_2, is the initial concentration of the I_2 solution,$C_{Na_2S_2O_3}$ *is the* concentration of sodium thiosulfate solution (mol/L),$V_{Na_2S_2O_3}$ is the volume of sodium thiosulfate solution (mL), V_{I_2} is the volume of iodine dosed (mL), M_{I_2} is the molar mass of iodine (g/mol), V_{ads} is the adsorption volume (mL) and m_{AC} is the mass of activated carbon(g).

Methylene blue number

The Methylene Blue Number (MBN) is defined as the maximum amount of dye adsorbed on 1g of adsorbent. Adsorption experiments of methylene blue molecules are easy and usually performed to characterize activated carbon with the aim of obtaining information about the adsorption capacity of materials. According to the dimensions of the methylene blue molecule, it is mostly adsorbed in mesopores, with the pores having a diameter of 20-500Å, so is related to the macro- and mesopore capacity of activated carbon [34].

The methylene blue number was calculated by the following equation:

$$MBN\left(\frac{mg}{g}\right)=\left(\frac{C_0MB-C_e}{m}\right)*V \quad (6)$$

here, C_0MB is the initial concentration of *MB* (mg/L), *Ce* is the equilibrium concentration of MB (mg/L), *M* is the mass of adsorbent (g) and *V* is the volume of the solution (L).

FTIR Analysis

The surface functional groups were studied by Fourier transform infrared spectrophotometer (FT-IR Perkin Elmer). A scan range of 400–4000 cm^{-1} was used to investigate the presence of functional groups on the surface of the prepared activated carbons.

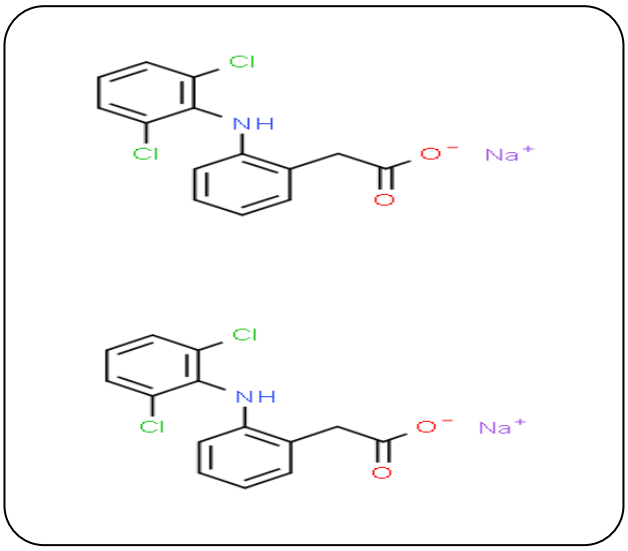

Fig. 2: Chemical structure of Diclofenac Sodic (DCF)

X-Ray Diffraction (XRD)

An X-Ray diffractometer was used to study the diffraction profiles of the activated carbons. Diffraction profiles were recorded for all samples using EMPYREAN PANALYTICAL with Ni filtered CuKα with radiation at 45KV and 40mA at a 0.02° step.

Scanning Electron Microscopy (SEM-EDS)

A scanning electron microscope was used to observe the surface pore structure of the prepared activated carbons. Micrographs of the morphology of the prepared activated carbons were measured by environmental scanning electron microscopy (Philips XL30 ESEM-FEG, EDS), (Energy Dispersive Spectroscopy) with an accelerating voltage of 20 kV.

Particle size distributions

Particle size distributions were measured using the HORIBA LA-960 Laser Scattering Particle Size Distribution Analyzer for Windows [liquid way] Ver8.00.

Interferometric microscopy or optical profilometer

The three dimensions of surface characteristics were determined using the BRUKER Contour GT-K0 optical profilometer, Z-Scan range 0.1nm to 10mm, and maximum scan speed 28.1µm/s.

Batch adsorption experiments

A standard stock solution of Diclofenac sodium (1000 mg/L) was prepared by dissolving the congruous amount in distilled water. The stock solution was then diluted to the desired concentration before the adsorption experiments. Batch adsorption studies were performed to determine the optimal mass of each activated carbon to determine the optimal parameters for adsorption of Diclofenac sodium. After stirring, the samples were centrifuged and filtered through a filter paper. The pH measurements were performed using HANNA instruments (HI 2211 pH/ORP Meter) and the equilibrium concentration of Diclofenac (Ce) was determined using a UV-Vis spectrometer (JASCO V-630 Spectrophotometer) at a wavelength of 273nm. The amount of adsorbed drug residue *qt* (mg/g) and removal efficiency *R* (%) by Ce were calculated according to the following equations:

$$R\% = \left(\frac{C_0 DCF - C_t}{C_0}\right) * 100 \quad (7)$$

$$qe\left(\frac{mg}{g}\right) = \left(\frac{C_0 - C_e}{W}\right) * V \quad (8)$$

Where $C_0 DCF$ is the initial concentration of *DCF* (mg/L), *Ce* is the equilibrium adsorbate concentration (mg/L), C_t is the concentration at a given time *t* (mg/L), *V* is the volume of adsorbate solution (L) and *W* is the weight of adsorbent (g). Fig. 2 shows the chemical structure of diclofenac sodic (DCF).

RESULTS AND DISCUSSION

Raw materials analysis

The results of the analysis of the sampled biomass are presented in Table 1.

The results of proximate analysis for different biomass samples are given in Table 1.

It appears from the immediate analysis that the moisture content which provides a lower value of 5% is considered correct according to the standards of activated carbons of the SNI n°06-3720-1995(table 2). The average moisture content of different biomass shown in Table 1, ranged from 2.69% to 10.92%. This shows that all samples were well dried and stored before collection, except for the typha briquettes which are outside the correct moisture range according to EN 14961-2 which should be below 10%. Charred walnut shells have the lowest moisture content with 3.5% (less than 5%).

The ash is the solid mineral matter that remains after the combustion of the walnut shell is of the order of 1.1, a minimum value compared to others biomass cited on Table 1, and according to the standard indicated in Table 2 are lower than 10%.

Table 1: Comparison of proximate analysis of Walnutshells with ACs prepared from various agricultural waste

Fuels	Moisture (%)	Volatile Matter (%)	Ash (%)	Fixed Carbon (%)	References
Wood charcoal (W.C)	5.05	39.94	7.05	53.01	[35]
Bamboo charcoal (B.C)	2.69	25.38	5.23	69.39	[35]
Bamboo biocharcoal (B.Bc)	4.66	30.36	7.99	61.65	[35]
Typha biocharcoal	5.66	52.95	43.22	3.83	[35]
Bioterre (peanut shell + clay)	3.00	42.00	55.27	2.73	[35]
Jatropha residues (J.R)	8.84	77.73	5.25	17.02	[35]
Shea butter cake pellets (S.B.C.P)	9.27	74.22	10.36	15.42	[35]
Typha pellets	8.61	87.89	6.33	5.78	[35]
Wood Pellets	7.44	84.89	0.07	15.04	[35]
Typha Briquettes	10.92	82.21	5.61	12.18	[35]
Peanut shell	7.01	80.55	3.32	16.13	[35]
Rice husk	5.88	63.92	22.90	13.18	[35]
Jute Stick	4.8	11.9	11.9	14.8	[36]
The Cones of Iranian Pine Trees (Pinus eldarica)	10.94	64.86	6.47	17.73	[37]
Durian HuskWastes	30.34	76.70	4.25	21.10	[38]
Powdered palma shells (PPS)	9.6	51.2	15	24.2	[39]
Walnut shells	3.5	1.97	1.1	96.92	This study

Table 2: Quality standards of activated carbon according to SNI (06 - 3730 - 1995)

No	Description	Unit	Requirements
1	Water content	%	Max.15
2	Ash	%	Max.10
3	Volatile Matter	%	Max.25
4	Fixed Carbon	%	Min.60
5	Moisture content	%	Max. 15
6	Iodine Adsorption	mg/g	Min.750

The Volatile Matter (MV) of all biomass shows that carbonized samples have the lowest MV rates, the case of our walnut shell (less than 25%). Uncharred samples especially densified ones have the best MV rates (above 80%).

The fixed carbon content varies widely among the above biomass. Bioterre has the lowest content (2.73%) and walnut shell charcoal has the highest content (96.92%). Our sample has a carbon content higher than 25%, the particularity is that our sample is only coal.

The low ash content may justify that the precursor is mainly organic matter and therefore has a high fixed carbon content. The rate volatile matter content of 1.97%has the advantage that the activated carbon has a high number of functional groups [40]. These results therefore suggest that walnut shells are suitable for the production of good activated carbon [41].

Material characterization

Iodine number

The adsorption capacity of iodine was affected by activated carbons produced at different concentrations of H_3PO_4 (Table 3). The results show that the iodine number of AC35% is much higher than the other concentrations of the activating agent. The higher iodine number of the activated carbon was attributed to the presence of a high micropore content which may have resulted from the reactivity of precursor material with theH_3PO_4activating agent.

Methylene blue number

The methylene blue index of the ACs at different concentrations of H_3PO_4 is presented in Table 3, it shows that the methylene blue index of AC35% is slightly higher than other activated carbons, this variation in the methylene blue index value is due to the different concentration of H_3PO_4. The higher methylene blue index of activated carbon was attributed to the presence of a large structure of mesopore and macropore which could be due to the reactivity of the activating agent H_3PO_4. It is clear that the uptake of methylene blue decreased by increasing surface area and % micropore volume but increased by increasing % mesopore volume. This indicates that the mesopore volume is more important than the micropore volume in this type of adsorption. According to Union of Pure and Applied Chemistry (IUPAC) the porous structures are divided based on pore diameter into micropores with a diameter < 2 nm, mesopores with diameters in the size of 2–50 nm, and macropores with diameters > 50 nm.

Table 3: Iodine and methylene blue numbers of Activated Carbons

Samples	AC20%	A C35%	AC40%	AC60%	AC75%	AC85%
Iodine number (mg/g)	2692.4	3784.6	2032	1981.2	1828.8	1016
Methylene blue number (mg/g)	1972.2	1990.67	1895.1	1904.68	1894.54	1819.31

Table 4: pHzpc values of activated carbons

Samples	AC20%	AC35%	AC40%	AC60%	AC75%	AC85%
pHzpc	5.6	4.9	2.2	2.2	2.2	4.4

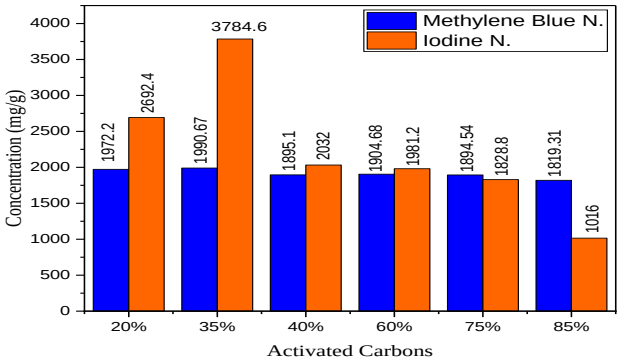

Fig.3: Comparison of iodine and methylene blue number

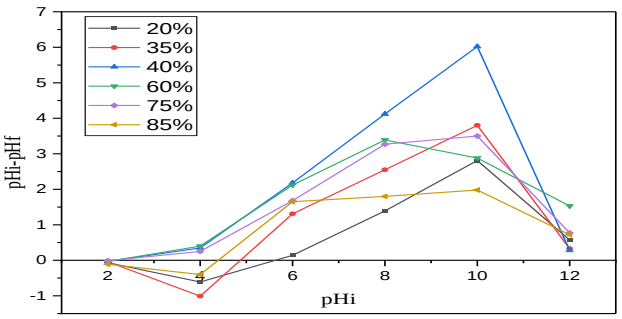

Fig. 4: Experimental determination of pHpzc of activated carbons at different concentrations of H_3PO_4.

Fig.3 shows the comparison of both the iodine number and methylene blue number for the activated carbons at different concentrations of H_3PO_4. It has been demonstrated how the iodine index and the methylene blue index can be used to estimate the surface area, micropore volume, and mesopore volume of activated carbon samples, so the highest values of both iodine value and methylene blue are observed in the AC35%.

Zero point charge pH (pH$_{ZPC}$)

The pH of zero-point charge (pH$_{ZPC}$) of different activated carbons with H_3PO_4 at different concentrations was obtained by constructing a graph of the difference between the initial and final pH of the solution (ΔpH) as a function of the initial pH, as shown in Fig.4.

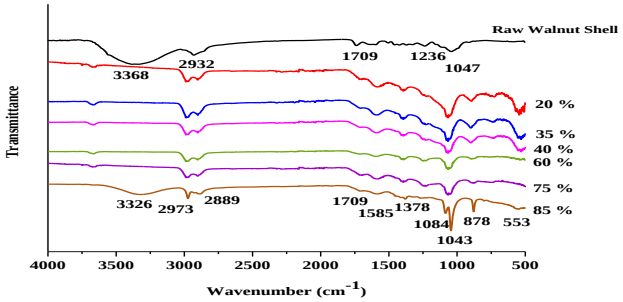

Fig.5: The FT-IR spectra of raw walnut shell compared with prepared activated carbons at different concentrations of H_3PO_4

According to the methodology proposed by *Noh* and *Schwarz* (1989) [42], the pH$_{PZC}$ corresponds to the region of the graph where the ΔpH is zero. We note that for all samples the pHpzc value, which happens to be the point of intersection with the abscissa, represents an acidic value.

The pHpzc value has a profound effect on how the pH of a solution can affect the adsorption process.

It can be seen in Table 4 that ACs contain similar acidic groups. These acidic groups comprise the phenol, lactone, and carboxylic groups. These results confirm that ACs exhibit acidic tendencies, as shown in Fig. 4. The pHpzc of activated carbons. The surface of activated carbons with pH values above pHpzc was protonated by the excess of H^+ ions, and the surfaces with pH values below pHpzc were deprotonated by the presence of OH^- ions in the solution. Thus, the groups on the surface of our CAs have an acidic character. This result was in fact predictable because the activating agent used is H_3PO_4 [43,44].

FT-IR analysis

FT-IR spectra of ACs derived from walnut shell at different concentrations of H_3PO_4 are shown in Fig. 5.

The raw walnut shell showed a complex FT-IR spectrum (Fig. 5), similar to lingo-cellulosic materials [45]. The strong broad band at 3368 cm^{-1} indicates O-H

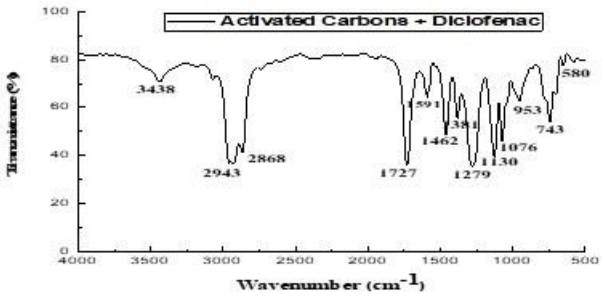

Fig.6: The FT-IR spectra of activated carbon after adsorption of Diclofenac

stretching vibration of hydroxyl groups. The band nearly at 2973 cm^{-1} can be assigned to C-H sp3 stretching bond of Alkane [46]. The bands at 1709 and 1585 cm^{-1} at the walnut shell spectrum can be attributed to the C=C stretching vibration of aromatic carboxyl groups [47]. The bands in the region between 1350 and 1380 cm^{-1} indicated C–O stretching in alcohol, carboxylic acid, esters, and ether [48]. Finally, the band at 553 cm^{-1} is described as O–H band [49].

Small absorption bands for ACs 20, 35, 40, 60, and 75% at 3669cm^{-1} and a wide band for AC85% with a maximum of 3326 cm^{-1} are attributed to bonded hydroxyl OH groups (alcohols, phenols, and carboxylic acids), or on the surface of ACs and of adsorbed water. An absorption band at 2973 and 2889 cm^{-1} Mainly resulting from aliphatic symmetric

and symmetricaliphatic C-H stretching vibrations in the Aromatic methoxy groups in the methyl and methylene groups in the sidechains, respectively. The peak at 1709cm^{-1} absorption band is attributed to the C=O stretching vibration of aryl, ketone or carboxyl groups [50,51]. The absorption band at 1585 $cm^{-1}$is attributed to the C=C stretching vibration of the aromatic benzene type. The absorption bands at 1448 cm^{-1} and 1411 $cm^{-1}$are attributed to the =C-H and C=C elongation vibration of aromatic benzene type, and to the =C-H in-plane deformation of the alkenes or O-H of phenol, respectively. An absorption band at 1268 cm^{-1} is attributed to the C-O-C asymmetric elongation of carboxylic acids, esters, or aryl class anhydrides. The bands at 1300 and 550 cm^{-1} are described in oxidized carbons and they are attributed to the elongation of C-O in acid, alcohol, phenol, ether, and ester groups but these bands are also characteristic of phosphorus and phosphor carbon compounds present in orthophosphoric acid activated carbons [52]. The absorption band at 1084 cm^{-1} an of C-O-C symmetric elongation of carboxylic acids, esters, or aryl class anhydrides and assigned to the stretching mode of P=O, O-C in P-O-C bonds and to P=OOH, is usually described and appears more intense when high concentrations of ACs are used [53-54]. The band detected at around1043 cm^{-1} is attributed to the ionized chemical bond P^{+}-O^{-} in acid phosphate esters [55-56] and to symmetric vibrations in P-O-P (polyphosphate) chains, to the vibrations of aliphatic P-O-C elongation or aromatic asymmetric elongation and P-OH deformation. The 878cm^{-1} band is attributed to C-P in phosphorus derivatives [57].

Nevertheless, the presence of all the functional groups of the different constituents is noted in each sample. As it can be seen, the most important changes in the activated carbons from walnut shells are due to the increase in the concentration of the activating agent. The development of the carbonyl groups and the increase of the content of phosphorous groups (1084, 1043, and 878cm^{-1}) which results in the intensification of the bands related to the phosphorous groups for AC 85% were clearly identified.Fig.6. Shows the FT-IR spectrum of AC after adsorption of DCF.

In order to determine the functional groups involved in the adsorption of (DCF) on CA, a comparison between FT-IR spectra before Fig. 5 and after adsorption Fig. 6 of DCF was made. The FT-IR spectra confirmed the changes in the functional groups and surface properties of the biosorbent. We observe the appearance of the same functional groups for both species before and after adsorption except for the FT-IR spectrum (B) after adsorption the appearance of N-H adsorption bands which confirms the successful incorporation of diclofenac groups. The absorption bands 3438cm^{-1} correspond to N-H free groups amide or amino. The stretching band and N-H wagging band are present at 1279 and 743 cm^{-1}, respectively, which confirms the successful incorporation of the NH_2 groups. The peaks at 953, 743, and 580 cm^{-1} of both materials (AC and DCF) are due to the vibrational group (CH) aromatic amine group (-NH). The FT-IR spectra of both materials are preserved.

XRD analysis

X-Ray Diffraction (XRD) patterns of all ACs show two broad humps revealing an amorphous structure. The crystalline structure for all samples is displayed

Table 5: EDS analysis of ACs

Elements / ACs	C (Wt%)	O (Wt%)	Na (Wt%)	Mg (Wt%)	SiK (Wt%)	S (Wt%)	P (Wt%)	Ca (Wt%)	Fe (Wt%)	Total
20%	64.44	24.98	3.14	0.81	-	-	3.77	2.39	0.48	100.00
35%	67.12	29.33	1.08	0.32	-	-	0.99	0.70	0.46	100.00
40%	68.63	28.15	1.03	0.29	0.17	-	1.04	0.68	-	100.00
60%	65.38	28.83	1.23	0.31	-	0.66	2.57	1.03	-	100.00
75%	70.22	27.10	0.93	0.35	-	0.06	0.65	0.42	0.26	100.00
85%	57.46	30.08	4.01	1.43	-	0.38	3.75	2.62	0.29	100.00

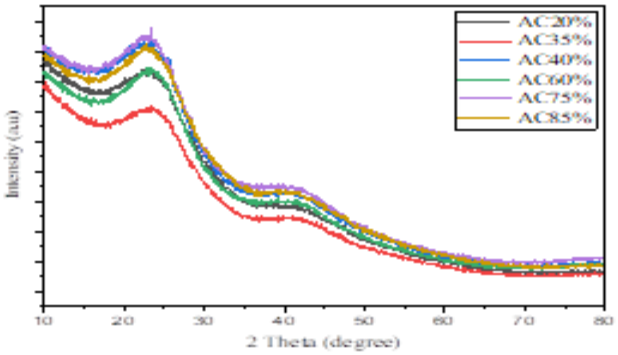

Fig.7: X-ray diffraction analysis of activated carbons

in Fig.7. Apparently, there are two wide humps, which are centered at about 23° and 43°. These two humps are belonged to (002) and (100) plane reflections of graphite, respectively [58]. The XRD patterns of all ACs samples reveal the absence of sharp and strong peaks, indicating the amorphous structure of activated carbons. The structures obtained in Fig. 7 have at most amorphous character. These characteristics permit to testing of the adsorption potential of ACs [59,60].

SEM-EDS analysis

Surface Morphology of activated carbons

The porous structure of the ACs shown in Fig. 8. The image shows the morphology of activated carbons at different concentrations of H_3PO_4. The surface morphology has a distinctive role in determining the adsorption zones, thus high surface areas increase the contact efficiency between the contaminants in solution and the ACs [61].

Considerable pores are distributed on the surface of all samples. It is clear that the pores were formed during the activation and carbonization steps. All images showed important porosity which increased by increasing the concentration of H_3PO_4 .The external surface of ACs is full of cavities and pores, the pores are formed and have different sizes and shapes with different amounts of the chemical agent H_3PO_4. These cavities were obtained by the vaporization of H_3PO_4 during the carbonization, leaving spaces that were occupied by the chemical agent [62-63].

The EDX spectrum of ACs samples by H_3PO_4shows in Fig. 9 intensity as a function of the energy (volt), the presence of a relatively large peak of C, which comes from the activated carbons EDX spectrum, indicates the presence of carbon, oxygen, sodium, magnesium, phosphorus, calcium, sulfur and iron.

Table 5 shows the elemental analysis of ACs, indicating the weight percentage of carbon, oxygen, sodium, magnesium, phosphorous, calcium, sulfur, and iron of the different activated carbons. These results contain the same elements as these studies' indifferent percentages [64-65]. Remarkably, the phosphorous in samples AC20, AC60, and AC 85% represents a high concentration and the shape of the spherical particles (Table 5)

Particle size distributions

Fig. 10 shows the particle size distribution of activated carbons, which was obtained by the laser diffraction particle sizer analyzer. The results show that all particles have average sizes between 3 and 50µm illustrated in Table 6 and a specific surface area between 1724.9 and 19375 cm^2/cm^3.

Table 6 shows the specific surface area and average diameter of all ACs, the lowest average diameter was 3.69µm for AC20% and the greatest average diameter was 49.77µm for AC35%, the greatest specific surface area 19375(cm^2/cm^3) for AC 85% and the lowest specific

Table 6: Granular characteristic of activated carbons prepared at different concentrations of H_3PO_4.

Samples	Average diameter (µm)	Sp ecific Surface (cm^2/cm^3)
AC20%	3.7	17063
AC35%	49.77	2799.1
AC40%	5.72	12116
AC60%	46.63	1724.9
AC75%	5.3	13327
AC85%	3.72	19375

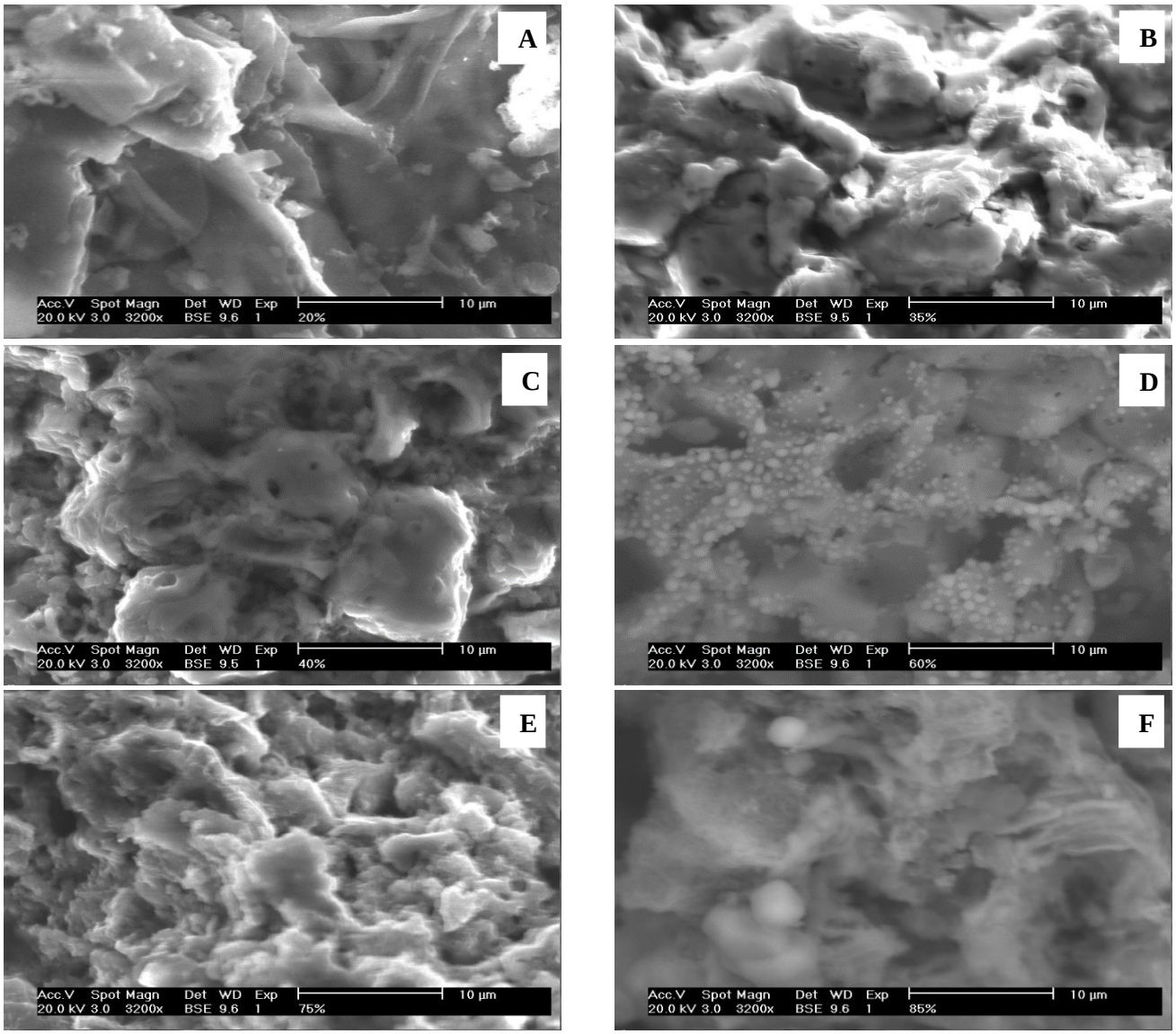

Fig. 8: SEM image of ACs with H_3PO_4 at different concentrations (20,35,40,60,75 and 85%)

surface area was 1724.9(cm^2/cm^3) for AC 60%. These results show the pore size distribution of the carbon samples, indicating that the samples have a broad pore size distribution, large mesopores and macropores. The peak in fig. 10 present [0-100µm] region indicates the mesopore and macropore region. A pore size distribution pattern is obtained in all samples.

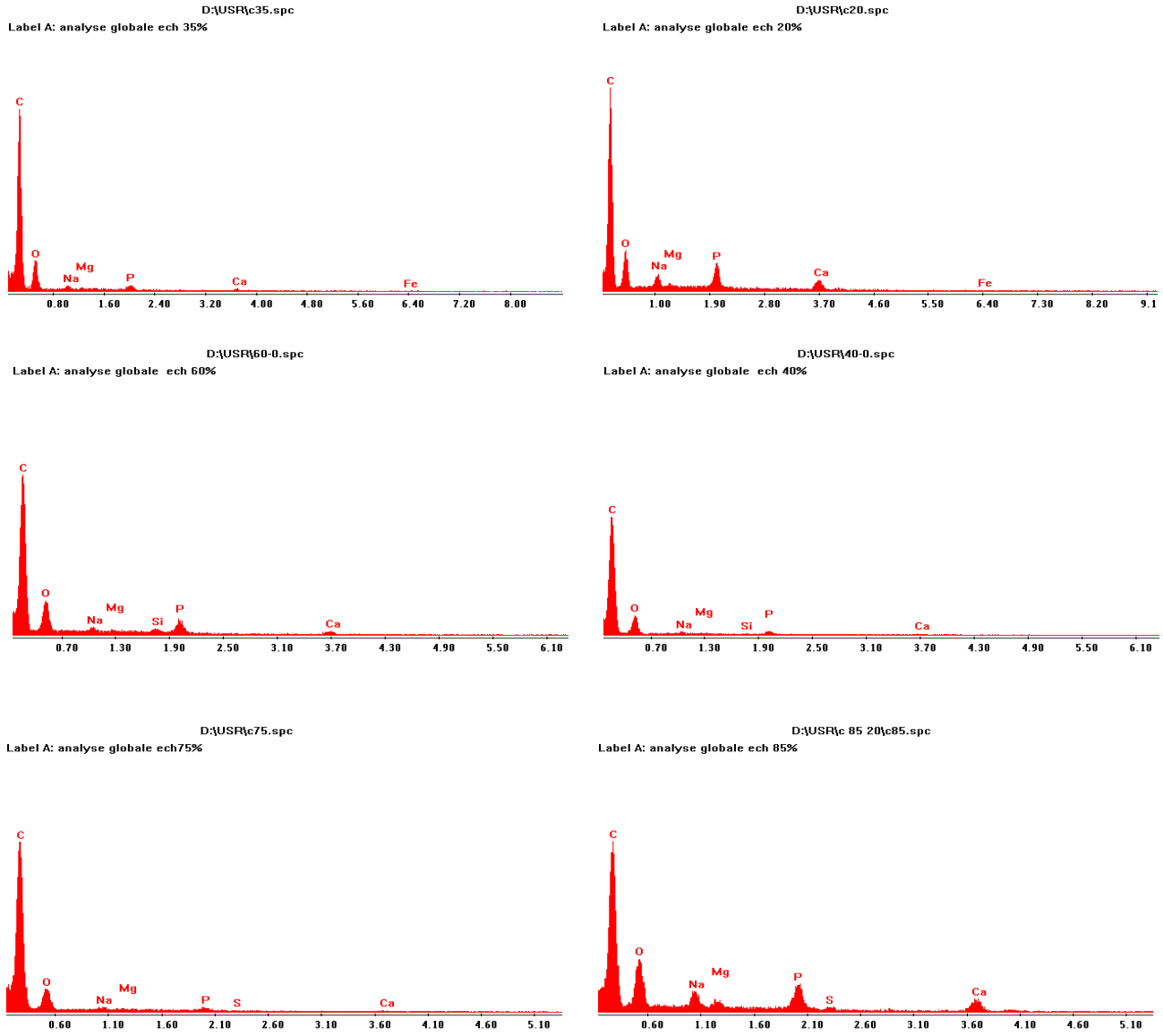

Fig. 9: EDS spectrum of all ACs, intensity as a function of the energy (volt)

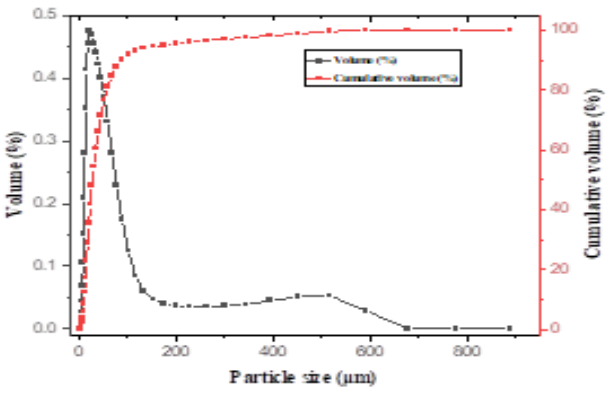

Fig. 10: Particle size distribution of AC35%

Interferometric microscopy

The interferometric Microscopy is an important method for surface characteristics that can measure and image surface characters in three dimensions, for a very broad range of surfaces, from nanoscale roughness to millimeter-scale elevations. Fig. 11 shows the interferometric images of the different ACs prepared from walnut shells at different concentrations of H_3PO_4. It is evident that the surface of all ACs were irregular, with a roughness greater than 90 µm. The table 7 shows the variations of the roughness for the different ACs and table 8 represents Roughness parameters of ACs.

Table 7: Variation of roughness for all ACs withH_3PO_4 at different concentrations

ACs (%)	AC20	AC35	AC40	AC60	AC75	AC85
Mean height (µm)	195.1	155.6	90.83	179.8	259.1	184.8
Minimum height (µm)	0.5245	0	0	0.08075	42.5	0.09485
Maximum height (µm)	732.6	736	568.5	711.7	844.1	848.1
Range (Min-Max) (µm)	732.1	736	568.5	711.6	801.6	848

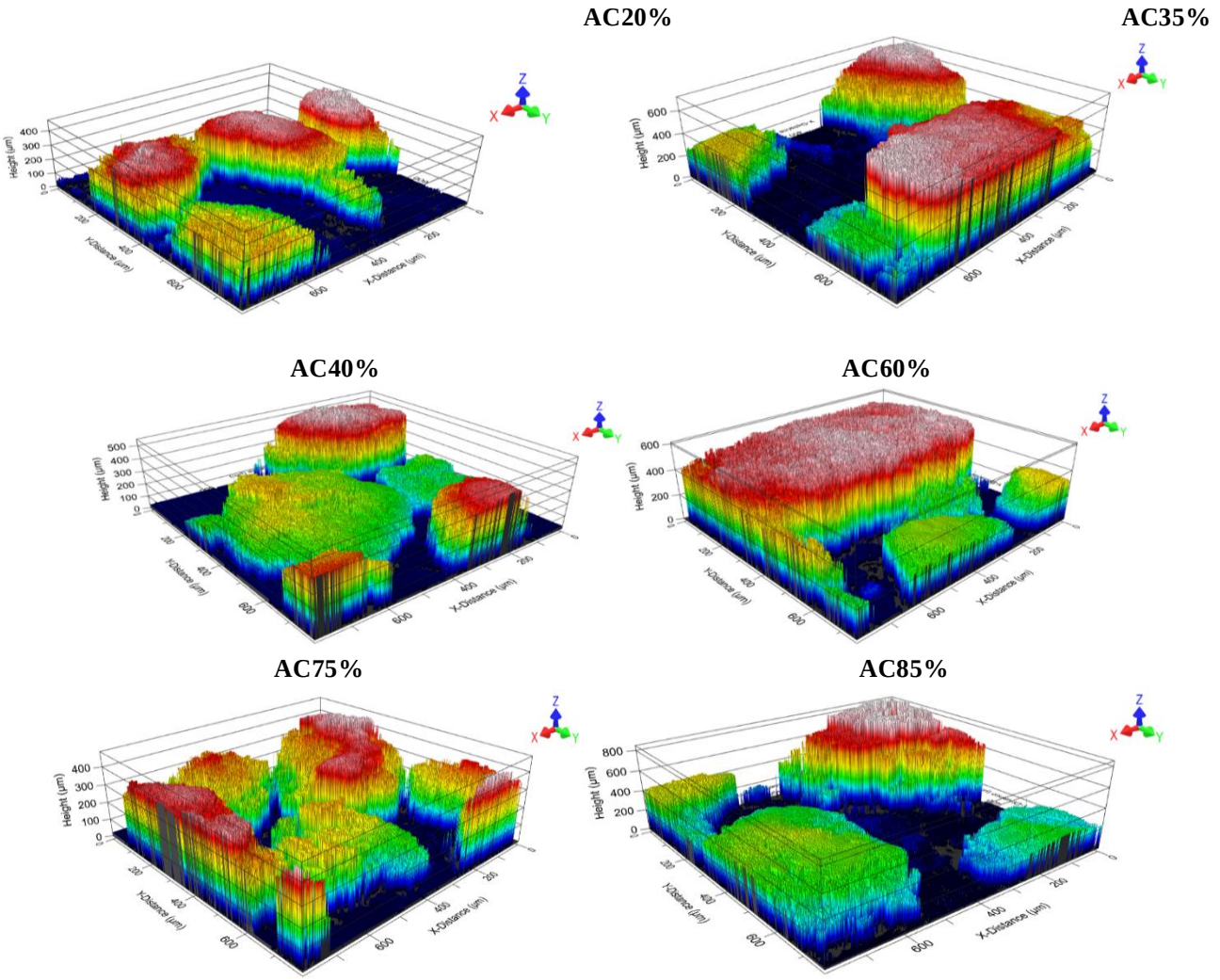

Fig.11: Optical profilometer of all ACs

The mean values of the six ACs area roughness are summarized in Table 7

We notice important values of the roughness up to 259.1 µm for AC75% this big value is due to the different concentrations of H_3PO_4 and the different diameters for each ACs. The roughness variation and 3D images clearly indicated the reactivity with the activating agent, and it is quite remarkable that the high particle height of all ACs. with increasing the concentration of activating agent until reaching a maximum height for AC85% is 848.1µm.

Roughness parameters

Obtaining a parameter that statistically represents all surface height differences is difficult and there are several parameters currently in use (root mean square variations, skewness, kurtosis and others). The roughness parameters for ACs according to the standard ISO 25178

Table 8 : Roughness parameters of ACs

	Sp (µm)	Sv (µm)	Sz (µm)	Sa (µm)	Sq (µm)	Ssk	Sku
AC20%	537.5	194.5	732.1	149.1	170.9	0.7953	2.735
AC35%	580.4	155.6	736	135.9	167.6	1.455	4.408
AC40%	477.7	90.83	568.5	93.57	122.4	1.864	5.299
AC60%	531.9	179.7	711.6	158.1	179	0.7718	2.298
AC75%	585	216.6	801.6	122.2	149.4	1.57	4.461
AC85%	663.3	184.7	848	191.3	219.2	1.005	2.878

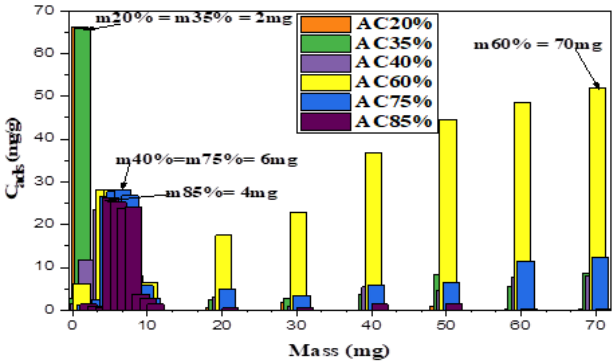

Fig. 12: Effect of which mass on the adsorption of Diclofenac at different concentrations of H_3PO_4.(C_0 = 70mg/L, mACs = 1-70mg, T = 298k, Agitation speed= 300rpm, pH =5.5, t = 1h)

Height are: Sp, Sv, Sz, Sa, Sq, Ssk and Sku. Three amplitudes (Sa, Sz, Sq), in this regard, the definitions of these parameters are: Sa is the arithmetic mean of the absolute values of the surface departures above and below the mean plane within the sampling area and represents an overall measure of the surface texture. Sq is similar to Sa and is the Root Mean Square (RMS) roughness. Sz maximum height is defined as the average value of the absolute heights of the five highest peaks and the depths of the five deepest pits or valleys within the sampling area. Sp is the maximum peak height, Sv is Maximum pit height, Ssk is the *Skewness* and *Sku* is *Kurtosis* [66].

The mean values of the roughness parameters are summarized in Table 8, the most representative parameter is Sz of the ACs. However, since these are deterministic surfaces with very large amplitudes, and considerable peak and pit heights [67].

Optimization parameters

Diclofenac (DCF) is a pharmaceutical nonsteroidal anti-inflammatory drug and is used in human medical care as an analgesic compound. Its chemical formula is $C_{14}H_{11}Cl_2NO_2$, its molar mass is 296.148 g/mol and its pKa is equal to 4.2, Many studies have used adsorption to remove diclofenac from aqueous solutions [68].

Effect of mass

The study of the influence of the activated carbon mass allows us to determine the most appropriate mass for an efficient adsorption in a range taken between 1-70mg. The results of the effect of the mass of the different samples on the adsorption of Diclofenac are presented in Fig. 12.

We find that for each sample, the maximum adsorption capacity increases to the maximum equilibrium concentration. This is due to the fact that the amount of adsorbate fixed must be in agreement with the dose of adsorbent in the solution to ensure an equivalent number of adsorption sites. Above a certain mass, a decrease is observed which may be due to another type of interaction between the adsorbate and the adsorbent. It could be a competition between the fibers retaining fractions of the pollutant and the free fibers of the adsorbent which attract it, making it return to solution [69].

Effect of pHi

The estimation of the pH of the most favorable medium for the adsorption of the different ACs has been evaluated and is presented in Fig. 13. We observe that for all the samples, the adsorption capacity of DCF decreases with the increase of the pH of the medium. This allows us to conclude that the adsorption of Diclofenac is favorable in acidic medium and for a maximum adsorption at pH = 2. These results can be explained by the London dispersion interactions that

predominate due to the non-dissociation of the adsorbate and the positive species on the adsorbent surface. However, at basic pH values, adsorption decreases due to electrostatic repulsions between the negative

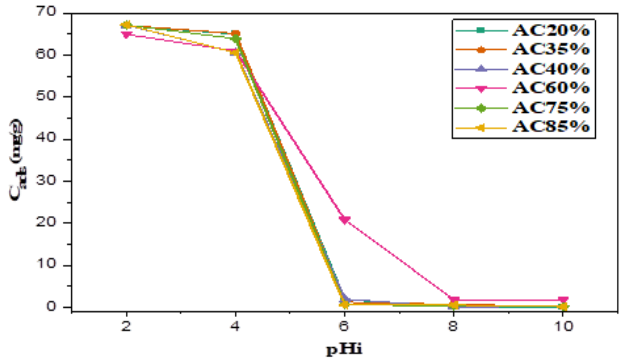

Fig.13: Effect of pHi on the removal efficiency of Diclofenac by activated carbons prepared from walnut shells. (C_0 = 70mg/L, T = 298k, Agitation speed = 300rpm, t = 1h, m_{CAs} = 2-70mg, pH = 2-10).

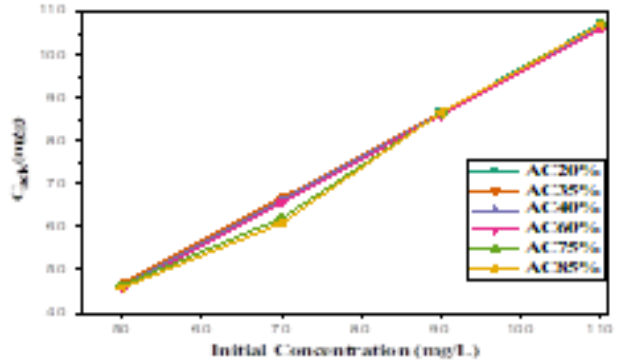

Fig. 14: Effect of initial concentration on the removal efficiency of Diclofenac by ACs prepared at different concentrations of H_3PO_4. (C_0 = 50-70mg/L, T = 298k, Agitation speed= 300 rpm, t = 1h, m_{CAs} = 2-70the range of experiments at pH=2

charges of the surface functions of the activated carbon and the anionic form of Diclofenac, as well as between the negatively charged ions of the active ingredient. The basic conjugated forms are the most important [69,70].

Effect of the initial concentration on the adsorption of Diclofenac

In all water treatment processes, the influence of the initial concentration of pollutants is of major importance. The results show in Fig. 14. that the amount of adsorbate attached increases with the increase of Diclofenac concentration in solution. This can be explained by the fact that the increase in concentration induces the elevation of the driving force of the concentration gradient, and thus the increase of the diffusion of the molecules in solution through the surface of the adsorbent [71].

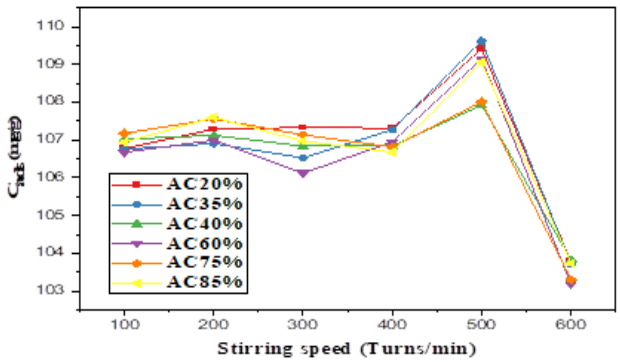

Fig. 15: Effect of stirring speed on the removal efficiency of Diclofenac by ACs prepared from walnut shells. (C_0 = 110mg/L, T =298k, Agitation speed=100-600rpm, t = 1h, m_{CAs} = 2-70mg, pH = 2).

Effect of stirring speed on the adsorption of Diclofenac

The effect of stirring speed is an important parameter of the liquid phase adsorption process. The effect of increasing the stirring speed of the solution for each sample from 100-600 rpm is plotted in Fig. 15. We can observe that the increase in turbulence has little impact on the adsorption capacity from 100 to 400 turns/min and then increase significantly at 500 rpm. This can be explained by the fact that the diffusion rate of drug molecules from the solution to the surface of the activated carbon increases due to the increase in turbulence leading to the decrease of the boundary layer around the adsorbent. This effect can also be explained by the fragmentation of the adsorbent particles making the surface more accessible [72]. However, we note a significant decrease in the adsorbed concentration of the pollutant by increasing the agitation speed to 600 turns/min. Indeed, authors have reported in their work that the adsorption increased with the increase of the stirring speed to a certain limit. In some cases, as here, the decrease in adsorption capacity is due to the fact that the kinetic energies of the adsorbate molecules and the adsorbent particles increase to the point where they collide, causing their detachment [73].

Effect of contact time on the adsorption of Diclofenac

The results of the adsorption of Diclofenac on activated carbons as a function of contact time are shown on fig.16. The experiments were performed to detect the time required for adsorption of Diclofenac sodium by ACs to reach equilibrium in time (0-140) min. The results showed higher adsorption in 60 min

Table 9: Percentages of removal of Diclofenac

Times \ ACs	AC20%	AC35%	AC40%	AC60%	AC75%	AC85%
t = 5 min	96.71%	96.8%	97.18%	96.9%	96.96%	96.82%
t = 15 min	94.59%	95.09%	94.31%	94.74%	94.55%	95.1%
t = 60 min	99.47%	99.66%	98.11%	99.22%	98.19%	99.14%

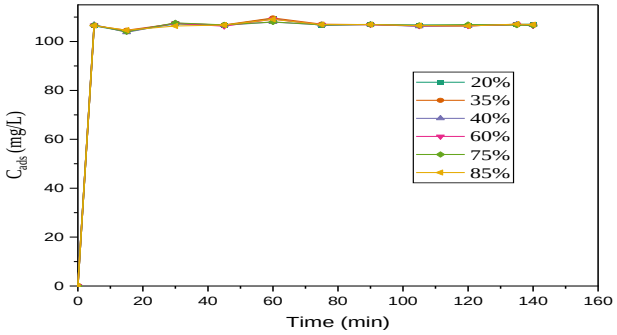

Fig. 16: Effect of time on the removal efficiency of Diclofenac by ACs prepared from walnut shells. (C_0 = 110mg/L, T =298k, Agitation speed=500 rpm, t = 05-140 min, m_{CAs} = 2-70mg, pH = 2).

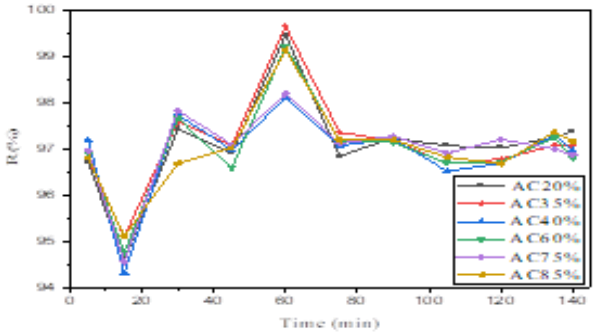

Fig. 17: Removal yield of Diclofenac by ACs with H_3PO_4 at different times

and equilibrium was at 5-140 min. In contrast, the highest adsorption of DCF by AC35% occurred in 60 min, (99.66%) [74]. The adsorbed concentration of Diclofenac increases between 15 and 30min and drops slightly at 45min to increase significantly for all CAs, and reaching a maximum peak at 60 min of contact time. Indeed, the molecules adsorb first on the easily accessible sites. A diffusion of these molecules will take place as the agitation proceeds toward the less accessible adsorption sites. A slight decrease in the adsorption capacity is noticeable after a contact time higher than the maximum reached at 60 min until reaching a stability level. Prolonged agitation leads to the desorption of molecules weakly bound to sites on the surface of the activated carbons [75].

It was observed that all ACs prepared to achieve a good removal yield of Diclofenac greater than 94%. Fig. 17 presents the removal percentage of this drug fluctuant from which the lowest value was attributed to AC40% with 94.31% at time 15min and the greatest value was attributed to AC35% at time 60 min with 99.66%.

Table 9 shows the initial, lowest, and highest removal efficiency of diclofenac by ACs at different concentrations of H_3PO_4 with contact time varying between 5 and 140min, the adsorption of Diclofenac starts at about 96.71% for AC20% at time 5min to decrease to 94.31% for AC40% at time 15 min and then increases to reach maximum adsorption at time 60min for AC35% with 99.66%.

Effect of temperature on the adsorption of Diclofenac

Increasing the temperature is known to increase the diffusion rate of adsorbate molecules through the outer boundary layer and into the interior of the adsorbent particles, due to the decrease in the viscosity of the solution [76]. Fig. 18 illustrates the effect of temperature on the adsorption capacity of Diclofenac. This Figure shows that the adsorbed quantity of DCF decreases with the increase in the temperature and the concentration of the activating agent. Therefore, a reduction of the adsorption capacity of Diclofenac. All samples show a minimum of adsorption capacity followed by a non-negligible increase of the adsorption capacity at low temperatures. According to adsorption theory, the adsorption decreases with increasing temperature and molecules adsorbed earlier on a surface tend to desorb from the surface at higher temperatures [77]. These results are consistent with the theory of adsorption. The decrease in adsorption capacity with increasing the temperature indicates that the process is exothermic, and would lead under these conditions to physical adsorption [78].

Table10: Comparison between the removal efficiency of this ACs with another adsorbent

Precursors	Agent activato rs	Pollutants and yield	Ref.
Rice Husk Residue	H_3PO_4	Landfill leachate over 90% high removal of TN 84% COD 82% NH_4^+–N 100%	[79]
Apricot stone	HCl	4-bromoaniline (4BA) 79%	[1]
Cherry stones	physical activation T= 600° C, at 4h	Congo Red (CR) ionic azo 99%	[80]
Sugarcane bagasse (SB)	dried in an oven at 60 °C for 24 h	Ciprofloxacin (CPX) 78%	[81]
-Phoenix dactylifera rachis (PRAC) - Ziziphus jujuba stones (JSAC) Palm rachis Palm rachis Commercial AC	 H_3PO_4 KOH KOH	eliminate a commercial reactive dye BEZAKTIV Red S-Max (BRSM) 48h PRAC 89.4% JSAC 73.6% 86.5 47.5 16.2	 [82]
Opuntia ficus indica	NaOH	p-nitrophenol, greater than 94%	[83]
Carbon fiber	La-OH doped	Phosphate 87%	[84]
Argan Nut Shell	H_3PO_4	Bisphenol 93%	[85]
Vitis vinifera leaf litter	H_3PO_4 ZnCl2	Aqueous phenanthrene 58.4% 47.08%	[86]
Walnut shells	H_3PO_4	Diclofenac sodium (DCF) 99.66%	This study

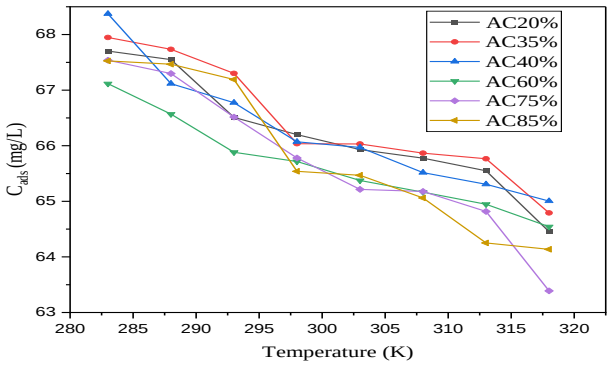

Fig. 18: Effect of temperature on the removal efficiency of Diclofenac by activated carbons prepared from walnut shells.(C_0 = 110mg/L, T = 283-318k, Agitation speed= 300 rpm, t = 1h, m_{CAs} = 2-70mg, pH = 2).

Table 10 shows the comparison between the removal efficiency of ACs from walnut shells with other adsorbents.

CONCLUSIONS

The impact of increasing concentrations on the pore structure and surface chemistry of activated carbons derived from walnut shells with the chemical activation method using phosphoric acid (H_3PO_4) as the activating agent for adsorptive removal of Diclofenac was studied. The Activated Carbons (ACs) were produced using different concentrations 20,35,40,60,75 and 85%, respectively, which are referred to as AC20, AC35, AC40, AC60, AC75 and AC85%. It was found from the results that a low concentration of 35% in H_3PO_4 promotes high adsorption of iodine index and methylene blue with 3784.6 and 1990.67mg/g, respectively, thus a maximum removal efficiency of DCF. However, the physicochemical characterization confirm that the prepared activated carbon has a large heterogeneous specific surface area and better adsorption capacity. The adsorption study was tested on pharmaceutical substance which is diclofenac sodium. The optimal condition of Diclofenac corresponds to the mass of AC35% of 2 mg, a maximum concentration of 110 mg/L, taken as the initial concentration in this work, pHi equal to 2, stirring speed of 500 rpm, contact time of one hour, and at room temperature. The results also showed that the percentage of DCF removal by ACs prepared from walnut shells, is in the order of more than 94% for all the samples of which AC35% in H3PO4, takes the lead with a yield of 99.66%and minimum with 98.11% for AC40%. The point of zero charge of all ACs had a distinct neutrality in acidic conditions, a factor that favors adsorption of cationic species within this pH range. The ACs prepared also had a high level of carbon content with low mineral content, making it ideal for application in water treatment or pharmaceutical wastewater treatment. The results of this study indicated that walnut shells can be turned into a useful product for drug release, this would specifically help to reduce the environmental cost of waste disposal.

Acknowledgments

The authors wish to express their thanks for the Direction Générale de la Recherche Scientifique et du Développement Technologique (DGRSDT), Algeria.

Received : Aug. 03, 2022 ; Accepted : Apr. 3, 2023

REFERENCES

[1] Tizi H., Berrama T., Hamane Dj., Ferrag-Siagh F, Bendjama Z., Characterization of New Adsorbent Prepared from Apricot Stones activated Carbon Mixed with Amorphous SiO_2 from Algerian Diatomite for Removal of p-Nitroaniline, *APTEFF*, **52**: 73-88, 1450-7188 (2021).

[2] Sekar M., Sakthi V., Rengaraj S., Kinetics and Equilibrium Adsorption Study of Lead (II) onto Activated Carbon Prepared from Coconut Shell, *J. Colloid Interface Sci*., **279**: 307–313 (2004).

[3] Dilek A., Production and Characterization of Activated Carbon from Sour Cherry Stones by Zinc Chloride, *Fuel*, **115**: 804–811(2014).

[4] Tzong-Horng L., Shao-Jung W., Characteristics of Microporous/Mesoporous Carbons Prepared from Rice Husk Under Base-and Acid-Treated Conditions, *Journal of Hazardous Materials*, **171(1-3)**: 693–703(2009).

[5] Al-Othman Z., A., Ali R., Naushad Mu., Hexavalent Chromium Removal from Aqueous Medium by Activated Carbon Prepared from Peanut Shell: Adsorption Kinetics, Equilibrium and Thermodynamic Studies, *Chemical Engineering Journal*, **184** :238–247(2012).

[6] Ghasemi M., Ghoreyshi A.A., Younesi H., Khoshhal S., Synthesis of a High Characteristics Activated Carbon from Walnut Shell for the Removal of Cr(VI) and Fe(II) from Aqueous Solution: Single and Binary Solutes Adsorption, *Iran. J. Chem. Chem. Eng. (IJCCE)*, **12(4)**: 28–51(2015).

[7] Martinez M.L., Torres M.M., Guzman C.A., Maestri D.M., Preparation and Characteristics of Activated Carbon from Olive Stones and Walnut Shells, *Industrial crops and products*, **23(1)**: 23–28 (2006).

[8] Qiongfen Y., Ming L., Xu J., Qiu Yu., Yuntao Z., CongbinLeng., Characterization and Methanol Adsorption of Walnut-Shell Activated Carbon Prepared by Koh Activation, *Journal of Wuhan University of Technology-Mater. Sci. Ed.,* **31(2)**: 260–268 (2016).

[9] Abdel-Nasser A., El-Hendawy A., Samra S.E., Girgis B.S., Adsorption Characteristics of Activated Carbons Obtained from Corncobs, *Colloids Surf. A: Physicochem. Eng. Asp.,* **180**: 209–221(2001).

[10] Kim J.W., Sohn M.H., Kim D.S., Sohn S.M., Kwon Y.S., Production of Granular Activated Carbon from Waste Walnut Shell and Its Adsorption Characteristics for Cu^{2+} ion, *J. Hazard. Mater*. **85**: 301–315(2001).

[11] Tsai W.T., Chang C.Y., Lee S.L. Preparation and Characterization of Activated Carbons from Corncob, *Carbon* **35**: 1198–1200(1997).

[12] Srinivasakannan C., Bakar M.Z.A., Production of Activated Carbon from Rubber Wood Sawdust, *Biomass Bioenergy*, **27**: 89–96 (2004).

[13] Hanedi E., Faten M., Mongi ben M., Ramzi K., Younes M., Biocarbon Derived from Opuntia Ficus Indica for p-Nitrophenol Retention, Processes, **8**: 1242 (2020).

[14] Guilaine J., Carla Patrícia S., João A.B.P. Oliveira, Sérgio M.S., María Victoria G., Marta O., Vânia C., Valdemar I.E., Production of Highly Efficient Activated Carbons from Industrial Wastes for the Removal of Pharmaceuticals from Water—A Full Factorial Design, *Journal of Hazardous Materials*, **370**: 212–218 (2019).

[15] Khadhri N., El Khames Saad M., ben Mosbah M., Moussaoui Y., Batch and Continuous Column Adsorption of Indigo Carmine onto Activated Carbon Derived from Date Palm Petiole, *Journal of Environmental Chemical Engineering*, (2018).

[16] Mongi ben M., Lassaad M., Ramzi K.,Younes M., Current State of Porous Carbon for Wastewater Treatment, *Processes*, **8**:1651(2020).

[17] Tizi H., Berrama T., Kaouah F. & Bendjama Z., Study of the Conditions of Activated Carbon Preparation from an Agriculture By-Product for 4BA Elimination in Aqueous Solution Using Full Factorial Design, *Desalination and Water Treatment*, **51**: 37-39 (2013).

[18] Rimene D., Mokhtar G., Murat Y., Lassaad M., Abdulmohsen Khalaf Dhahi A., Fathi A., Ridha Ben S., Younes M., Experimental Design Analysis of Murexide Dye Removal by Carbon Produced from Waste Biomass Material, *Journal of Chemistry*, Article ID 9735071 **1**: (2022).

[19] N'guessan Louis Berenger K., Koffi P., Dit A., N'goran Luc D.B., D.D. T.A., Simultaneous Removal of Copper and Lead from Industrial Effluents Using Corn Cob Activated Carbon, *Chemistry Africa* https://doi.org/10.1007/s42250-022-00432-2 (2022).

[20] Zhang, N., et al., Photodegradation of Diclofenac in Seawater by Simulated Sunlight Irradiation: The Comprehensive Effect of Nitrate, Fe(III) and Chloride, *Marine Pollution Bulletin*, (2017).

[21] Nan Z., Guoguang L., Haijin L., Yingling W., Zhanwei H., Gang W., Diclofenac Photodegradation Under Simulated Sunlight: Effect of Different Forms of Nitrogen and Kinetics, *J. Hazard. Mater*., **192**: 411-418 (2011).

[22] Tahereh S.h., Minoo T., Amitav A., Arne T., Reinhard Schomäc K., Michael S., Impact of Operating Conditions for the Continuous-Flow Degradation of Diclofenac with Immobilized Carbon Nitride Photocatalysts, *J. Photochem. Photobiol. A: Chem.*, **388**: 112182 (2022).

[23] Ling F., Eric D. Van H., Manuel A., Rodrigo Giovanni E., Mehmet A.O., Removal of Residual Anti-Inflammatory and Analgesic Pharmaceuticals from Aqueous Systems by Electrochemical Advanced Oxidation Processes, A Review, *Chem. Eng. J.*, **228**: 944–964 (2013).

[24] Bénilde B., Elena G., Frédérique C., Aurélie E., Hélène F., Diclofenac in the Marine Environment: A review of its Occurrence and Effects, *Mar. Pollut. Bull*., 1–28 (2018).

[25] Mohd R., Neetu G., A QM/MM Study to Investigate Selectivity of Nanoporous Graphene Membrane for Arsenate and Chromate Removal from Water, *Chem. Phys. Lett.*, **685**: 371-376 (2017).

[26] Zeid A. ALOthman Ahmad Yacine B., Omar M.L., Alharbi I.A., Synthesis of Chitosan Composite Iron Nanoparticles for Removal of Diclofenac Sodium Drug Residue in Water, *Inter. J. Biol. Macromol.*, **159**: 870-876 (2020).

[27] Ozlem O., Cetin K., Diclofenac Removal by Pyrite-Fenton Process: Performance in Batch and Fixed-Bed Continous Flow Systems, *Sci. Total Environ.*, **664**: 817-823(2019).

[28] Zahra Shams-G., Alireza Nezamzadeh-E., As-synthesized ZSM-5 Zeolite as a Suitable Support for Increasing the Photoactivity of Semiconductors in a Typical Photodegradation Process, *Mater. Sci. Semicond. Proc.*, **39**: 265-275 (2015).

[29] Hu Z., Srinivasan M.P., Ni Y., Novel Activation Process for Preparing Highly Microporous and Mesoporous Activated Carbons, *Carbon*, **39**: 877–886 (2001).

[30] Sudaryanto Y., Hartono S.B., Irawaty W., Hindarso H., Ismadji S., High Surface Area Activated Carbon Prepared from Cassava Peel by Chemical Activation, *Bioresour. Technol*., **97**: 734–739 (2006).

[31] Ahmadpour A., Do D.D., The Preparation of Active Carbons from Coal by Chemical and Physical Activation, *Carbon*, **34**: 471–479 (1996).

[32] Franz M., Arafat H.A, Pinto N.G., Effect of Chemical Surface Heterogeneity on the Adsorption Mechanism of Dissolved Aromatics on Activated Carbon, *Carbon*, **38**: 1807–19(2000).

[33] ASTM. "Standard Test Method for Determination of Iodine Number of Activated Carbon", 1, ASTM International, **94** :1–5 (2006).

[34] Rapaso F., De La Rubia M.A., Borja R., Methylene Blue Number as Useful Indicator to Evaluate the Adsorptive Capacity of Granular Activated Carbon in Batch Mode: Influence of Adsorbate/Adsorbent Mass Ratio and Particle Size, *Journal of Hazardous Materials*, **165(1–3)**: 291–9(2009).

[35] André N., Pierre W. Tavares, Aliou S., Moustapha K., Hawa N., Issakha Y., Proximate Analysis of Alternatives Cooking Solides Fuels in Sub Saharan by Using Astm Standards, I*nternational Journal of Clean Coal and Energy*, **11**: 1-12 (2022).

[36] Arshad Hussain W., Inam Ullah W., Abdul Manan W., Preparation and Characterization of Rice Husk Based Physical Activated Carbon, *Energy Sources, Part A: Recovery, Utilization, and Environmental Effects*, (2020).

[37] Soheil V., Habibollah Y., Nader B., Preparation and Characterization of Activated Carbon from the Cones of Iranian Pine Trees (Pinus eldarica) by Chemical Activation with H_3PO_4 and Its Application for Removal of Sodium Dodecylbenzene Sulfonate Removal from Aqueous Solution, (2018).

[38] Tongsai J., Nitchanan I., Nattharika K., Kemmika P., Wasana Sr., Rattanaphol M., Piyada W., Kun-Yi Andrew L., Chih-Feng H., Study of the Enhancements of Porous Structures of Activated Carbons Produced from Durian Husk Wastes, *Sustainability*, **14**: 5896 (2022).

[39] D E.E., N.R.P., Shehata N., Preparation and Characterization of Powdered and Granular Activated Carbon from Palmae Biomass for Cadmium Removal, *International Journal of Environmental Science and Technology*,**17**: 2443–2454 (2020).

[40] Mbaye G., Développement De Charbon Actif A Partir De Biomasse Lignocellulosique Pour Des Applications Dans Le Traitement De L'eau, *Thèse de doctorat en technologie de l'Eau, de l'Energie et de l'Environnement, 2iE, Burkina Faso*, **215**: (2014).

[41] Siragi D.B., Maazou., Halidou I.H., Malam Alma M.M, Amadou Z., Natatou I., Elimination Du Chrome Par Du Charbon Actif Elaboré Et Caractérisé A Partir De La Coque Du Noyau De Balanites Aegyptiaca, *Int. J. Biol. Chem. Sci.*, **11(6)**: 3050-3065(2017).

[42] Noh**,** J.S., Schwarz, J.A., Estimation of the Point of Zero Charge of Simple Oxides by Mass Titration, *J. Colloid Interface Sci.*,**130**: 157–164 (1989).

[43] Marzbali M.H., Esmaieli M., Abolghasemi H., Marzbali M.H., Tetracycline Adsorption by H_3PO_4 Activated Carbon Produced from Apricot Nut Shells: A Batch Study, *Process Safety and Environmental Protection*, **10**: 2700–709 (2016).

[44] Kodama S., Sekiguchi H., Estimation of Point of Zero Charge for Activated Carbon Treated with Atmospheric Pressure Non-Thermal Oxygen Plasmas, *Thin Solid Films*, **506** – **507**:327 – 330 (2006).

[45] Nour T., Abdel G., Ghadir A, Chaghaby E.l., Mohamed H., El Gammal, El Shaimaa A.R., Optimizing the Preparation Conditions of Activated Carbons from Olive Cake Using KOH Activation, *New Carbon Materials*, **31(5)**: 492–500 (2016).

[46] Azmi N., Ali U., Ridwan F., et al., Preparation of Activated Carbon Using Sea Mango (Cerbera Odollam) with Microwave-Assisted Technique for the Removal of Methyl Orange from Textile Wastewater, *Desalination and Water Treatment*, **57(60)**: 29143–29152 (2016).

[47] Hashemian S., Salari K., Salehifar H., et al., Removal of Azo Dyes (Violet B and Violet 5R) from Aqueous Solution Using New Activated Carbon Developed from Orange Peel, *Journal of Chemistry*, **2013**: 1–10 (2013).

[48] Moreno-Barbosa J.J, López-Velandia C., Maldonado A.D.P, et al., Removal of Lead (II) and Zinc (II) Ions from Aqueous Solutions by Adsorption onto Activated Carbon Synthesized from Watermelon Shell and Walnut Shell, *Adsorption*, **19(2-4)**: 675–685 (2013).

[49] Fan L., Chen J., Guo J., et al., Influence of Manganese, Iron and Pyrolusite Blending on the Physiochemical Properties and Desulfurization Activities of Activated Carbons from Walnut Shell, *Journal of Analytical and Applied Pyrolysis*, **104(11)**: 353–360 (2013).

[50] Guo Y., Rockstraw D.A., Physical and Chemical Properties of Carbons Synthesized from Xylan, Cellulose, and Kraft Lignin by H_3PO_4 Activation, *Carbon*, **44**:1464–1475(2006).

[51] Boonamnuavitaya V., Sae-ung S., Tanthapanichakoon W., Preparation of Activated Carbons from Coffee Residue for the Adsorption of Formaldehyde, *Sep. Purif. Technol.*, **42**: 159–168 (2003).

[52] Solum M.S., Pugmire R.J., Jagtoyen M., Derbyshire F., Evolution of Carbon Structure in Chemically Activated Wood, *Carbon*, **33(9)**: 1247–54 (1995).

[53] Puziy A.M., Poddubnaya O.I., Martınez-Alonso A., Suarez-Garcıa F., Tascon J.M.D., Synthetic Carbons Activated with Phosphoric Acid - I. Surface Chemistry and Ion Binding Properties, *Carbon*, **40**: 1493–1505 (2002).

[54] Puziy A.M., Poddubnaya O.I., Martınez-Alonso A., Suarez-Garcıa F., Tascon J.M.D., Surface Chemistry of Phosphorus-Containing Carbons of Lignocellulosic Origin, *Carbon*, **43**: 2857–2868 (2005).

[55] Zawadzki J., Infrared Spectroscopy in Surface Chemistry of Carbons, In: Thrower P.A., Editor. "Chemistry and Physics of Carbon", New York: Marcel Dekker; **21**: 147-386(1989).

[56] Vinke P., Van Der Eijk M., Verbree M., Voskamp A.F., Van Bekkum H., Modification of the Surfaces of a Gas Activated Carbon and a Chemically Activated Carbon with Nitric Acid, Hypochlorite, and Ammonia, *Carbon*, **32(4)**: 675–86(1994).

[57] Socrates G., "Infrared Characteristic Group Frequencies", New York: John Wiley & Sons Inc., (1994).

[58] Ali N. et al., Thermodynamic, Kinetic and Isotherm Studies of Sulfate Removal from Aqueous Solutions by Graphene and Graphite Nanoparticles, *Desalination and Water Treatment* (2017).

[59] Abdul Khalil H.P.S., et al., Activated Carbon from Various Agricultural Wastes by Chemical Activation with KOH: Preparation and Characterization, *Journal of Biobased Materials and Bioenergy* (2013).

[60] Kong W., Zhao F., Guan H., Zhao Y., Zhang H., ZhangB., Highly Adsorptive Mesoporous Carbon from Biomass Using Molten-Salt Route, *J. Mater. Sci.*, **51**: 6793–6800 (2016).

[61] GadkareeK.P., JaroniecM., Pore Structure Development in Activated Carbon Honeycombs, *Carbon*, **38**: 983-993 (2000).

[62] Saygılı H., Güzel F., Onal Y., Conversion of Grape Industrial Processing Waste to Activated Carbon Sorbent and its Performance in Cationic and Anionic Dyes Adsorption, *J. Cleaner Product*., **93**: 84-93(2015).

[63] Hesas R.H., Arami-Niya A., Wan Daud W.M.A., Sahu J.N., "Preparation and Characterization of Activated Carbon from Apple Waste by Microwave-Assisted Phosphoric Acid Activation: Application in Methylene Blue Adsorption," *Bioresources*, **8**: 2950-2966 (2013).

[64] Allwar Allwar, Preparation and Characterizations of Activated Carbon from Banana Fruit Bunch with Chemical Treatments Using Hydrothermal Processes, *AIP Conference Proceedings 2229*, (2020).

[65] Mohammed Yahya M.S., Jeyashelly A., Zaidi A.G., A Preliminary Study on the Preparation of Activated Carbon from Cyrtospermachamissonis Petioles *via* Single Step H_3PO_4 Activation, *Applied Mechanics and Materials*, **799-800**: 47-51(2015).

[66] Emmanouil T., Eleana K., George V., Konstantinos A. Ioannis T., Surface Characterization of Monolithic Zirconia Submitted to Different Surface Treatments Applying Optical Interferometry and Raman Spectrometry, *Dental Materials Journal*, **39(1)**: 111–117 (2020).

[67] Beitia C., Abdel sater M., Cordeau M., Godny S., Petitgrand S., Alliata D., "Optical Profilometry and AFM Measurements Comparison on Low Amplitude Deterministic Surfaces", 978-1-5386-7601-1/19/ (2019) IEEE.

[68] Poorsharbaf G., Fatemeh R., Fereshteh D., Koohi, A., A Review on Diclofenac Removal from Aqueous Solution, Emphasizing on Adsorption Method, *Iran. J. Chem. Chem. Eng. (IJCCE)* **39(1)**: 1-14 (2020).

[69] Belaid D.K., Kacha S., Étude Cinétique et Thermodynamique de l'adsorption d'un Colorant Basique Sur La Sciure de Bois, *Revue des Sciences de l'Eau. Journal of Water Science*, **24(2)**: 1-15(2011).

[70] Daoud M., Benturkı O., L'Activation d'un Charbon à Base de Noyaux de Jujubes et Application à l'Environnement. Adsorption d'un Colorant de Textile., Le 3ème Séminaire International sur les Energies Nouvelles et Renouvelables (2014).

[71] Deniz F., Saygideger S.D., Investigation of Adsorption Characteristics of Basic Red 46 onto Gypsum: Equilibrium, Kinetic and Thermodynamic Studies, *Desalination*, **262**: 161-165(2010).

[72] Kuśmierek K., Świątkowski A.,The Influence of Different Agitation Techniques on the Adsorption Kinetics of 4-Chlorophenol on Granular Activated Carbon, *Reaction Kinetics, Mechanisms and Catalysis*, **116**: 261–271(2015).

[73] Jamil N., Ahsan N., Munawar M.A., Anwar J., Shafique U., Removal of Toxic Dichlorophenol from Water by Sorption with Chemically Activated Carbon of Almond Shells a Green Approach, *J. Chem. Soc. Pak*, **33**: 640–645 (2011).

[74] Bayan A.M., Anwar A.M., Zuhair A.A., Asaad M.R.A., Biosorption of Lead from Industrial Wastewater Using Some Part of Date Palm Trees, *Copyright © EM International*, **38 (4)**: 853-860 (2019).

[75] Anand N., Sellakutti N., Selvaraju S., Gajendiran V., Natesan S., Ahmad Hosseini-B., Preparation and Characterization of Cassava Stem Biochar for Mixed Reactive Dyes Removal from Simulated Effluent, Desalination Publications 1944-3994/1944-3986 (2020).

[76] Dogan M., Alkan M., Demirabas O., Ozedemie Y., Ozemetin C., Adsorption Kinetics of Maxilon Blue GRL onto Sepiolite from Aqueous Solution, *Chemical Engineering Journal*, **124**: 89-101(2006).

[77] Michael H.J., Ayebaemi I.S., Effects of Temperature on the Sorption of Pb^{2+} and Cd^{2+} from Aqueous Solution by Caladium Bicolor (Wild Cocoyam) Biomass, *Electronic Journal of Biotechnology*, **8:(**2) (2005).

[78] Pathania D., Sharma S., Sing P., Removal of Methylene Blue by Adsorption onto Activated Carbon Developed from Ficus Caricabast, *Arabian Journal of Chemistry*, 1-7 (2013).

[79] Yiping L., Dong L., Yichao C., Xiaoying S., Qin C., Xiaofeng L., "The Performance of Phosphoric Acid in the Preparation of Activated Carbon-Containing Phosphorus Species from Rice Husk Residue, Springer Science+Business Media", LLC, Part of Springer Nature (2018).

[80] Cristina-Gabriela G., Andrei-Ionuț S., Lidia F., Lucian G., Congo Red Removal from Aqueous Effluents by Adsorption on Cherry Stones Activated Carbon, *Grigoraș et al./Environmental Engineering and Management Journal*, **19**: 2,247-254 (2020).

[81] María E., Peñafiel José M., Matesanz E.V., Daniel B., Rosa M., Ormad M.P., Comparative Adsorption of Ciprofloxacin on Sugarcane Bagasse from Ecuador and on Commercial Powdered Activated Carbon, *Science of the Total Environment*, **750**: 141498 (2021).

[82] Mounir D., Oumessaâd B., Pierre G., André D., Sébastien F., Adsorption Ability of Activated Carbons from Phoenix Dactylifera Rachis and Ziziphus Jujube Stones for the Removal of Commercial Dye and the Treatment of Dyestuff Wastewater, *Microchemical Journal*, **148**: 493-502 (2019).

[83] Hanedi E., Faten M., Mongi ben M., Ramzi Kh., Younes M., Biocarbon Derived from Opuntia Ficus Indica for P-Nitrophenol Retention, *Processes*, **8**: 1242 (2020).

[84] Ling Z., Qi Zh., Jianyong L., Ning C., Lihua W., hydroxide-Doped Activated Carbon Fiber, *Chemical Engineering Journal*, 185–186, 160–167 (2012).

[85] Mohamed Z., Kaisu A., Asmaa D., Satu O., Michael B., Minna P., Riitta L. KEISKI, Mohammed B., Rachid B., Toward New Benchmark Adsorbents: Preparation and Characterization of Activated Carbon from Argan Nut Shell for Bisphenol A Removal, *Environmental Science and Pollution Research* (2017).

[86] Adetunji Ajibola A., Beatrice Olutoyin O., Olalekan Siyanbola F., Olushola Sunday A., Vanessa Angela J., and Reinette S., Preparation and Characterization of Activated Carbon from Vitis Vinifera Leaf Litter and its Adsorption Performance for Aqueous Phenanthrene, *Awe et al. Appl. Biol. Chem.*, **63**:12 (2020).